Int. J. Heat Mass Transfer. Vol. 28, No. 6, pp. 1131–1146, 1985
Printed in Great Britain

0017–9310/85 $3.00 + 0.00
Pergamon Press Ltd.

On the flow field generated by a growing sphere near a solid plane with application to nucleate boiling

M. A. ABDELGHAFFAR and K. CORNWELL
Heriot-Watt University, Edinburgh

(*Received* 18 *September* 1984 *and in final form* 7 *December* 1984)

Abstract—An exact analytical solution for the potential flow produced by a spherical cavity growing in contact with, or close to, a solid plane is described. The flow field parameters are given in a non-dimensionalised form and their characteristics are examined. The theory is applied to the case of an idealised nucleate boiling bubble. Expressions are obtained for bubble departure, pressure distribution around the bubble surface and, on the solid plane, the effect of bubble translation along the solid plane on flow parameters and the total kinetic energy imparted to the liquid. The concept of an 'area of influence' in nucleate boiling is reviewed. It is shown that neither this area nor the hydrodynamic effect inside it due to bubble motion, remain constant during bubble growth. Where possible, the results are compared with experimental data.

INTRODUCTION

THE STUDY of a growing or collapsing spherical-cavity in the vicinity of a plane solid surface is relevant to nucleate boiling, cavitation, gas dissolution in liquids and various other physical phenomena. A more comprehensive literature survey and detailed analysis of this problem are given in ref. [1]. Here, a brief account will be given.

Kotake [2], considers the case of a bubble in the shape of a truncated sphere growing on a solid plane surface. As pointed out in [3], the given solution does not satisfy the prescribed boundary conditions and does not predict the spherically symmetric result when the geometry is reduced to that of a hemisphere. This problem has since been reviewed by Abdelghaffar [1] and a solution satisfying the prescribed boundary conditions and predicting the spherically symmetrical case is obtained. Witze *et al.* [3], use a tangent-sphere coordinate system to solve Laplace's equation for the case of a growing sphere in contact with a solid plane. The exact solution is given in integral form. However, the integral does not seem to lend itself to analytic solutions. They propose an approximate solution which introduces some errors in calculating the velocity components. The error is greatest for the tangential velocity component. Judd [4], in a study aimed at evaluating inertia effects, obtains an expression for the velocity potential describing the field due to the motion of a spherical bubble moving perpendicular to a solid plane. The solution fails when the bubble is very close to the solid plane. Best *et al.* [5], model a bubble on its upward journey, perpendicular to a solid plane, by a doublet and a spatial source and their images in the plane. A correction term is added to allow for the shear forces at the solid surface; the method fails when the bubble is close to or in contact with the solid plane. The solution given by Barakat [5], for the case of a bubble in contact with a solid plane is not valid as pointed out in ref. [1]. Barakat also gives a solution, based on the method of multiple reflections, describing the motion of a spherical bubble of a constant size. Obviously this solution cannot be used for a growing or a collapsing bubble. Nigmatulin [7] uses the method of binary correlation functions, previously used [17] to determine the rate of settling of homogeneous suspensions, to calculate the average flow about a bubble (assuming that all bubbles have the same size). A solution, at low volumetric concentration of bubbles, for the case of two-phase flow in pipes is presented. The case of two bubbles, of the same size and rate of growth on a solid plane is treated in ref. [1].

2. BASIC ASSUMPTIONS AND PROBLEM FORMULATION

It is assumed that the fluid is inviscid and incompressible and that the flow is irrotational. At points far removed from the spherical cavity, the fluid is assumed to be at rest. The assumption that a bubble remains spherical in shape throughout its motion is reasonable for bubbles of relatively small size, under conditions of reduced gravitational force or where the surface tension is high enough. According to ref. [8], the bubble remains nearly spherical when the Eötvos number, $E\ddot{O}$, defined by

$$E\ddot{O} = \frac{2gR^2(\rho_L - \rho_g)}{\sigma} \tag{1}$$

is close to, or less than, unity.

The solid plane representing the heating surface in a boiling regime is assumed to be very large compared to the size of bubble. Although a boundary-layer correction is applied to the case of a bubble translating in a direction normal to the solid plane, it will be assumed here that the solid plane does not support any tangential shearing forces.

NOMENCLATURE

(r, ψ, Z) cylindrical coordinates with respect to fixed frame of reference
(r_0, ψ_0, Z_0) cylindrical coordinates with origin at centre of sphere or bubble
(ρ, θ, ψ) spherical coordinates with respect to a fixed frame of reference
$(\rho_0, \theta_0, \psi_0)$ spherical coordinates referred to centre of bubble or sphere
A_b fraction of heat transfer area due to boiling, equation (5)
a a constant
b a constant of a nucleate boiling regime, equation (A18)
C a constant depending on the fluid being boiled, equation (A20)
C_f a force factor, equations (A46) and (A74)
C_l specific heat of the fluid
$E\ddot{O}$ Eotvos number, equation (1)
$\mathbf{e}_r, \mathbf{e}_z$ unit vectors in the direction of r and z respectively
E_e total kinetic energy of the liquid, equation (A52)
E_{ep} kinetic energy of a particle having the same mass as that of the fluid displaced by the bubble and moving with a velocity equal to the bubble's growth rate
E_e^* normalized value of E_e, equation (A54)
$\mathbf{F}_n$ force acting on the bubble surface due to the pressure distribution over the surface, equation (A42)
F_b force acting on the bubble surface due to the pressure distribution over the surface, equation (A45)
f_p pressure factor, equation (A45)
g acceleration due to gravity
H height of sphere or bubble centre above solid plane
H^* H/R
h_{fg} latent heat of vapourization
J_a Jacob's number, equation (5)
K_1 ratio of influence area to projected area of bubble at departure equation (5)
m constant, equation (A69)
M_1 mass of equivalent particle
n' growth index, equation (A17)
p static pressure of liquid
p_∞ static pressure at infinity (points far away from bubble)
Δp $p - p_\infty$
$\mathbf{q}$ fluid velocity vector
q_r, q_z, q_ψ components of $\mathbf{q}$ in the direction of suffix
q_ρ, q_θ components of q in the direction of suffix
R radius of sphere or bubble
$\dot{R}$ dR/dt
$\ddot{R}$ $d\dot{R}/dt$
s surface area
t time
t_d bubble departure time
T_l absolute temperature of the fluid
T_d absolute superheat temperature of the fluid at the system pressure
$\mathbf{V}$ velocity vector describing the motion of centre of sphere or bubble
V_r, V_z components of $\mathbf{V}$ in the direction of the suffix
V_z terminal velocity of bubble.

Greek symbols
α_L thermal diffusivity of fluid
δ hydrodynamic boundary-layer thickness
λ z/δ
ν_L kinematic viscosity of the fluid
ρ_L, ρ_g liquid and gas densities respectively
ε $(\rho_L - \rho_g)/\rho_L$
Φ scalar potential function.
σ surface tension

Superscripts
$*$ normalized quantities
$\cdot$ d/dt.

Subscripts
o, c centre of sphere or bubble
d departure.

The continuity equation for an incompressible fluid takes the form

$$\nabla \cdot \mathbf{q} = 0 \tag{2}$$

where $\mathbf{q}$ is the velocity vector describing the fluid motion outside the bubble.

Since the flow is irrotational, the flow field can be described in terms of a scalar potential function, Φ, given by

$$\mathbf{q} = -\nabla\Phi. \tag{3}$$

Thus, whether the flow is steady or not, equations (2) and (3) give

$$\nabla^2\Phi = 0. \tag{4}$$

The solution of equation (4), subject to the appropriate boundary conditions, is given in ref. [1]. In the Appendix, the equations describing the flow field due to a non-spiralling motion of a spherical bubble, assumed to be the same as that of a spherical cavity, are given. The two important cases of a bubble moving perpendicular to the solid plane and that of a bubble growing on the plane (with or without translation) are treated in some detail.

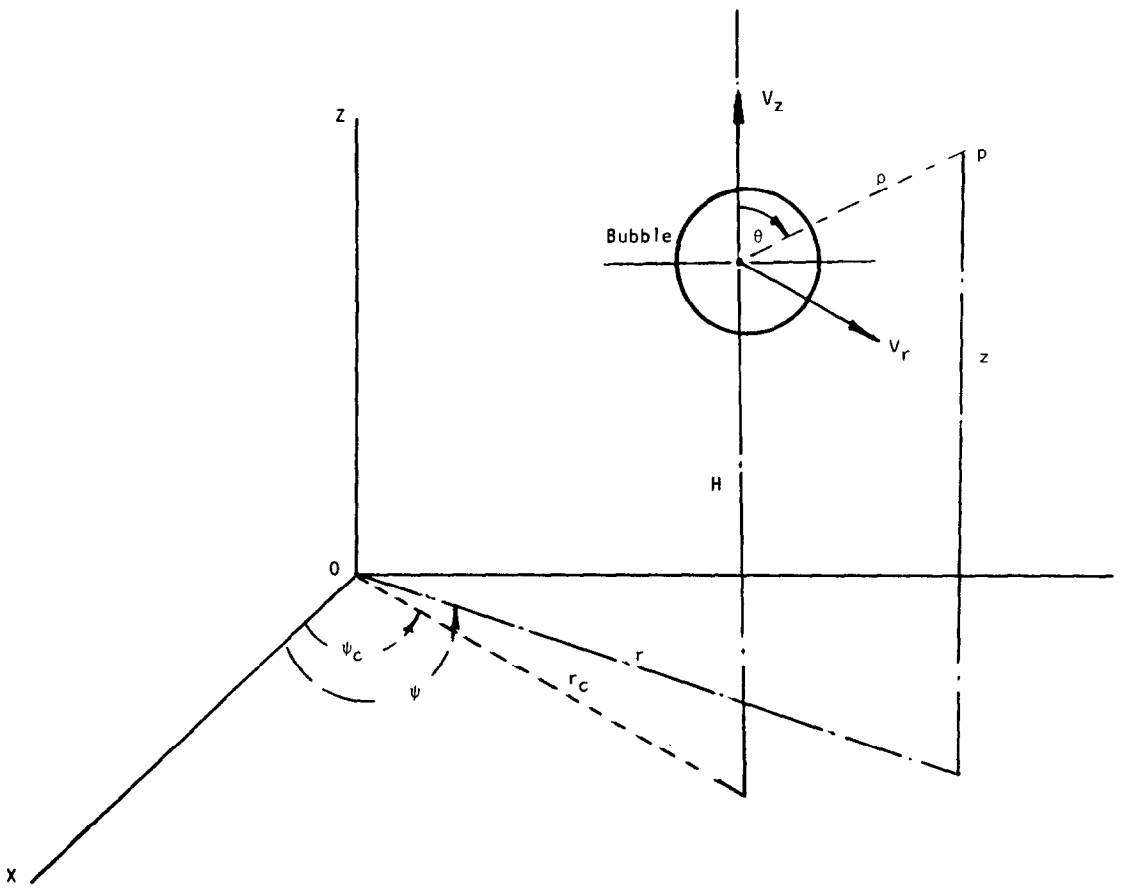

FIG. 1. Non-spiralling motion of bubble (see Appendix).

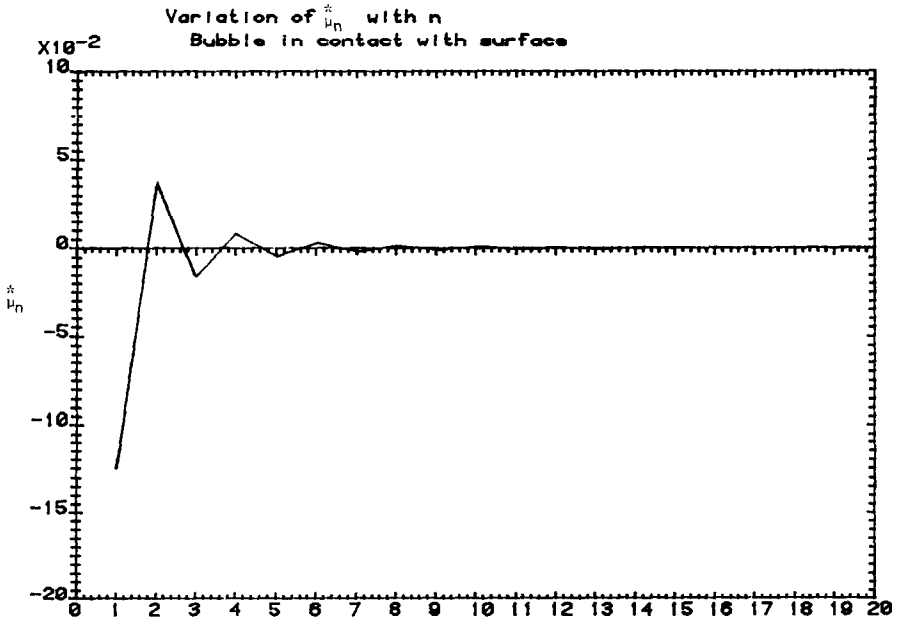

FIG. 2. Variation of μ_n^* with n. Bubble in contact with surface (see Appendix).

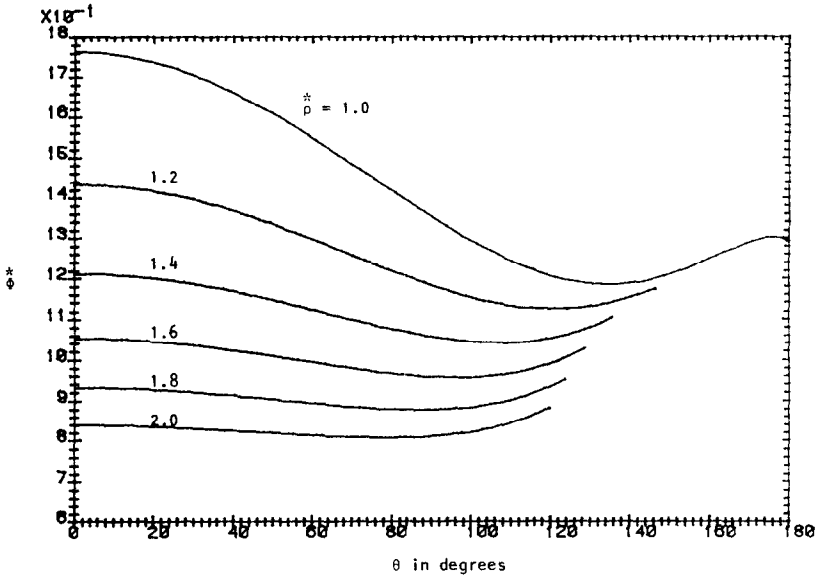

FIG. 3. Variation of potential function with position ($H^* = \varepsilon = 1$).

3. DISCUSSION

Figures 3–7 show some of the flow field characteristics for a spherical bubble growing on a solid plane without translation. Some of the properties of the flow field due to a spherical bubble translating on a solid plane are shown in Figs. 8–11. Figure 12 shows the variation of $\Delta P/\rho_L$ at a nucleation site for different values of the bubble height H while Fig. 13 shows the variation of $\Delta P/\rho_L$ on the solid plane for the same bubble 2 ms after its departure. The bubble, the field characteristics of which are depicted in Figs. 12 and 13, is assumed to be moving in water at 100°C, with $n = 0.5$ and $b = 0.0081$. The height of the bubble centre and its velocity have been calculated using equations (A20) and (A21) respectively while the fluid velocities used in equation (A35) have been calculated using equation (A23). Figures 14 and 15 show a comparison between theoretical results for the horizontal velocity com-

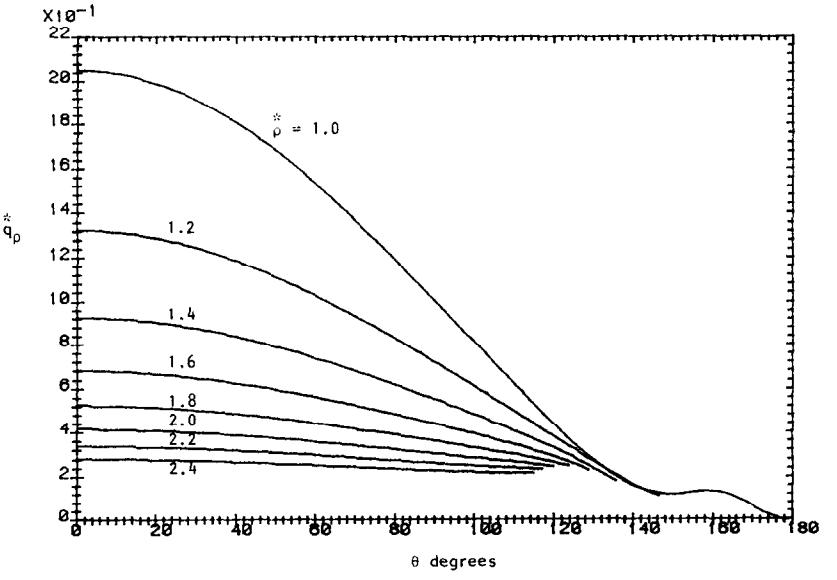

FIG. 4. Variation of normal velocity with position ($H^* = \varepsilon = 1$).

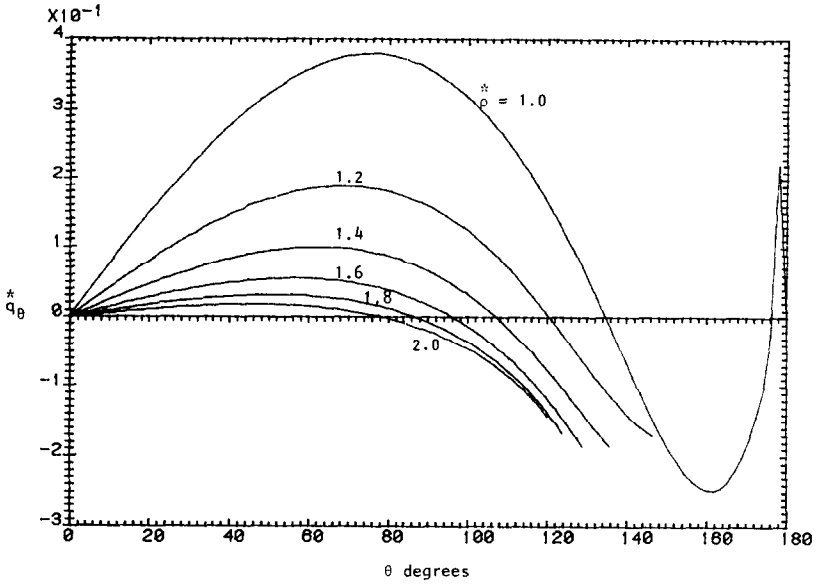

FIG. 5. Variation of tangential velocity with position ($H^* = \varepsilon = 1$).

ponent, calculated using equation (A23), and experimental values for two barbotage bubbles given in refs. [11] and [1]. (Barbotage is the bubbling of gas in liquids.)

Figure 3 shows the variation of the potential function, Φ^*, with (ρ^*, θ). It can be seen that Φ^* varies considerably over the bubble surface ($\rho^* = 1$). As ρ^* increases the variation of Φ^* with θ becomes less pronounced and reaches an almost constant value for $\rho^* = 2.5$. On the bubble surface, Φ^* shows a minimum at θ nearly 137°. At this point $q^*_\theta = 0$, as can also be seen in Fig. 5. Near the solid plane, the slope for Φ^* increases rather steeply which results in $q^*_\theta < 0$ (see Fig. 5). This causes fluid from regions close to the bubble base to be pushed towards the bubble equator. However, this effect is restricted to the region $137° < \theta < 176°$ as illustrated in Fig. 5. On the bubble surface Fig. 5 shows that q^*_θ is positive in the region $176° < \theta < 180°$ indicating that the fluid is being pushed in towards the bubble base. In practice this behaviour will be reduced due to the shearing forces at the solid wall. In the region $0° < \theta < 137.5°$, the fluid on the bubble surface moves from the top towards the bottom of the bubble. This can have a pronounced effect on the rate of bubble growth. As soon as the top part of the bubble penetrates the layer of superheated liquid, adjacent to the heated

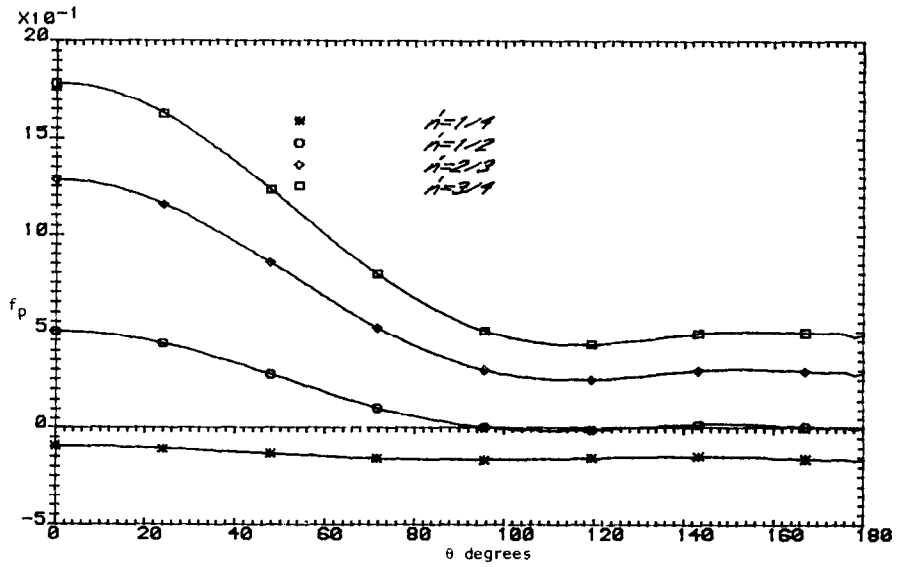

FIG. 6. Pressure factor vs θ on bubble's surface. Bubble in contact with surface ($\varepsilon = 1$).

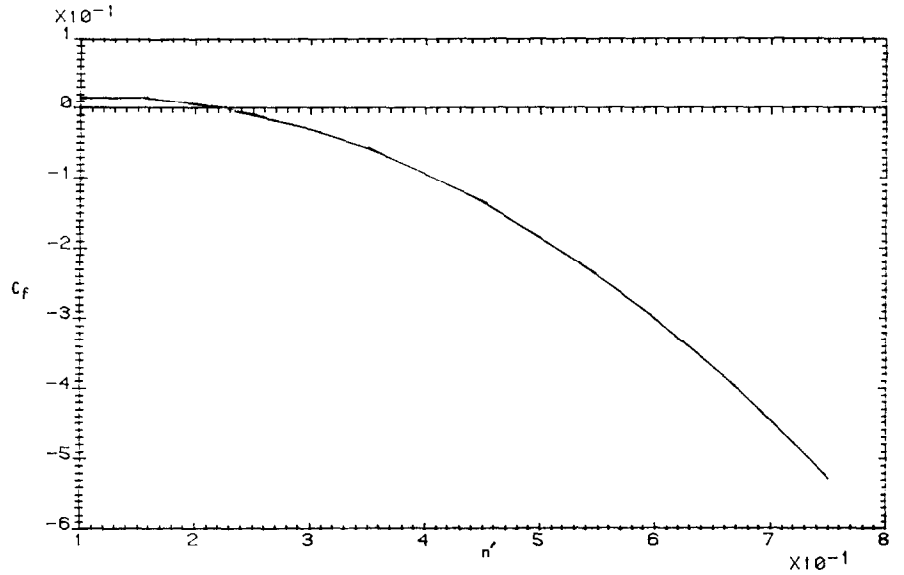

FIG. 7. Thrust coefficient C_f vs growth index n' ($H^* = \varepsilon = 1$).

surface to which it is attached, cooler liquid is pushed towards the bubble base. This hydrodynamic action may lead to the retardation of bubble growth rates or bubble implosion. Although at a distance approximately 2.5 times the bubble radius the normalized velocity components tend to a relatively small fraction of their values in the immediate vicinity of the bubble, these velocities depend on the bubble growth rate and may still have an important effect on the heat transfer mechanism. Thus during the early stages of bubble growth, when R is small and $\dot{R}$ is large, one is speaking about a large effect spread over a relatively small area. On the other hand, just before departure R is relatively large and $\dot{R}$ is small, so one is concerned with a small effect spread over a relatively wider area. In nucleate boiling an influence area is defined as that region within which the bubble activity affects the heat transfer mechanism and outside which natural convection prevails. The heat transfer area is divided into a boiling fraction A_b, and a natural convection fraction $(1 - A_b)$. The expression for the boiling fraction, A_b, is given by:

$$A_b = n_s(\pi R_d^2)K_i \tag{5}$$

where n_s is the nucleation site density, R_d is the departure radius and K_i is the ratio of influence to projected area of bubble at departure. Thus the value of K_i depends on R and is time dependent. Averaged values of K_i have been given by several authors, refs.

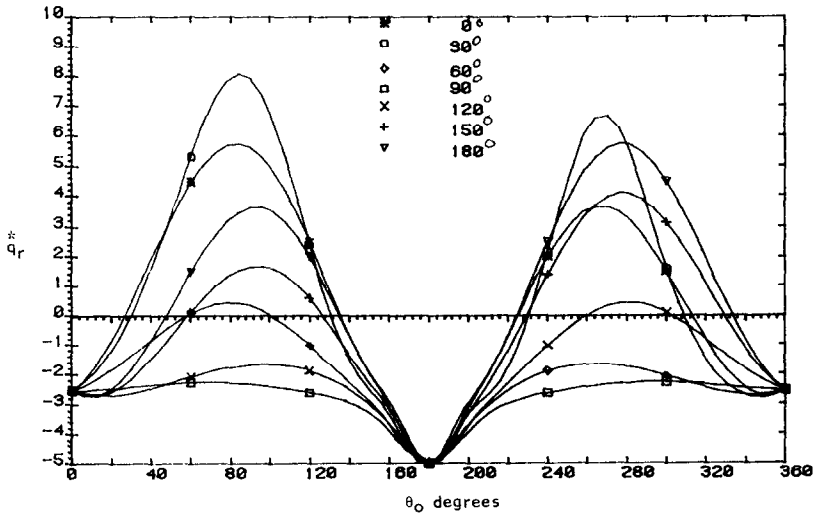

FIG. 8. Horizontal velocity for sliding bubble. $m = 5.0$, $\varepsilon = \rho_0^* = 1.0$. Values of ψ_0 given in legend.

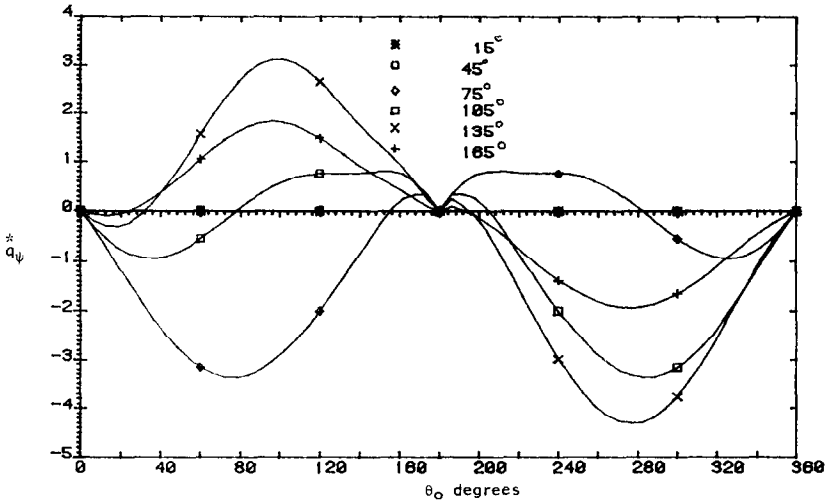

FIG. 9. Angular velocity for sliding bubble. $m = 5.0$, $\rho_0^* = \varepsilon = 1.0$. Values of ψ_0 given in legend.

[12] and [13], and ranges from 1.5 to 2.24 times the bubble radius. It is not the intention here to discuss these in any detail. However, the concept of an area of influence as defined above does not provide information about the fluid movement inside that area which varies directly with dR/dt. Thus although for large bubbles A_b is large, the effect due to bubble activity may be quite small for very low values of dR/dt.

It is also worth noting that although q_θ^* tends to zero for values of $\theta < \pi/3$ and $\rho^* = 2.5$, yet it is negative for values of $\theta > \pi/3$. This means that the fluid is being pushed away from the wall at a rate which may affect the convective heat transfer mechanism and growth of other bubbles over distances considerably larger than is generally believed and by magnitudes much larger than would be the case for a slower growing bubble.

It must be remembered that for an imploding (collapsing) bubble the value of $\dot{R}$ is negative. This phenomenon usually occurs in subcooled regimes. For this case, the effect will be opposite to that described for a growing bubble in as far as signs of quantities are concerned. In this case the fluid close to the bubble location moves away from the wall while that some distance away from the bubble moves towards the wall thus forming a 'convective cell'. The reversal of the liquid motion, both on the bubble surface and in its vicinity, plays a crucial part in the mechanism of nucleate boiling as it affects heat transfer from the superheated thermal boundary layer adjacent to the wall and the bubble on one hand, and the thermal boundary layer and the liquid bulk on the other hand.

The pressure factor, f_p, on the bubble surface has

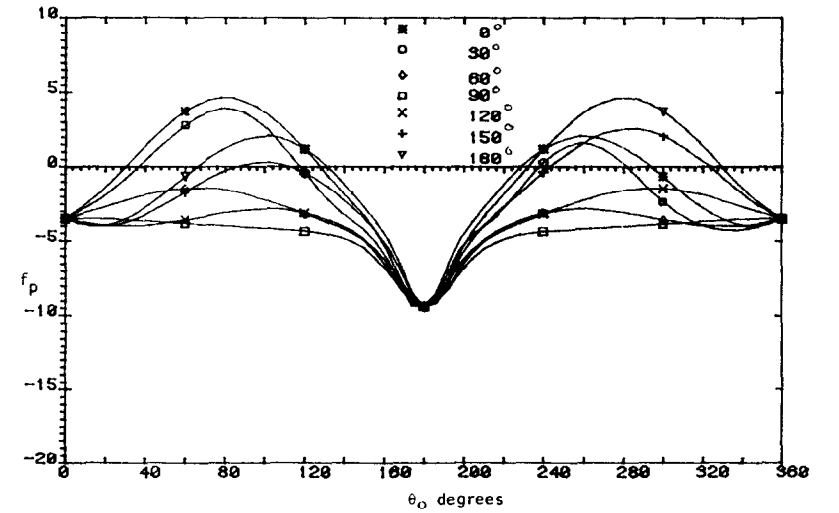

FIG. 10. Pressure factor for sliding bubble. $m = 5.0$, $n' = \frac{1}{2}$, $\rho_0^* = \varepsilon = 1$. Values of ψ_0 given in legend.

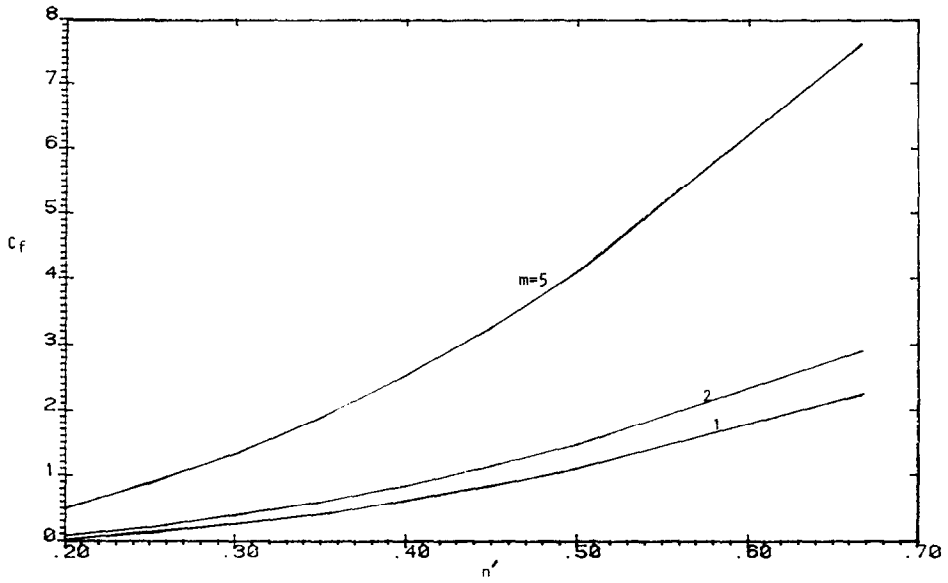

FIG. 11. Thrust coefficient for sliding bubble. $\varepsilon = 1.0$.

been calculated for different values of the growth index n' and the result is shown in Fig. 6. From this figure it can be seen that f_p is very sensitive to variations in the growth index n'. In all cases of n' considered, the maximum value of f_p, and hence Δp, occur at the bubble top. For $n' = 1/4$ the value of f_p remains almost uniform while the degree of variation from top to bottom becomes more pronounced as n' increases.

Figure 7 shows the variation of the thrust coefficient, C_f, with the growth index n'. From this it can be seen that for a value of n' less that about 0.23, C_f is positive and hence the pressure distribution tends to produce a repulsive force, rather than a restraining one. Examination of Fig. 6 reveals that Δp is negative for this range of n'. This implies that such bubbles will be collapsing (negative values for $\dot{R}$). Thus under conditions of strong subcooling leading to bubble collapse shortly after their initial growth to some size, it

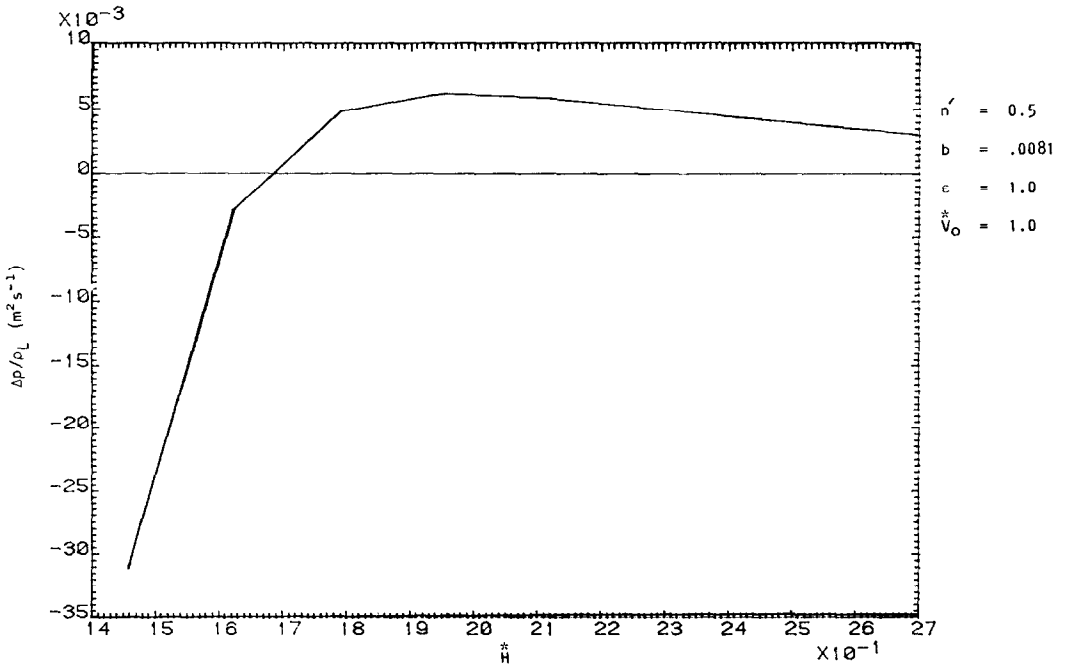

FIG. 12. Variation of Δp vs H^* at nucleation site. Initial velocity equal to rate of growth at departure.

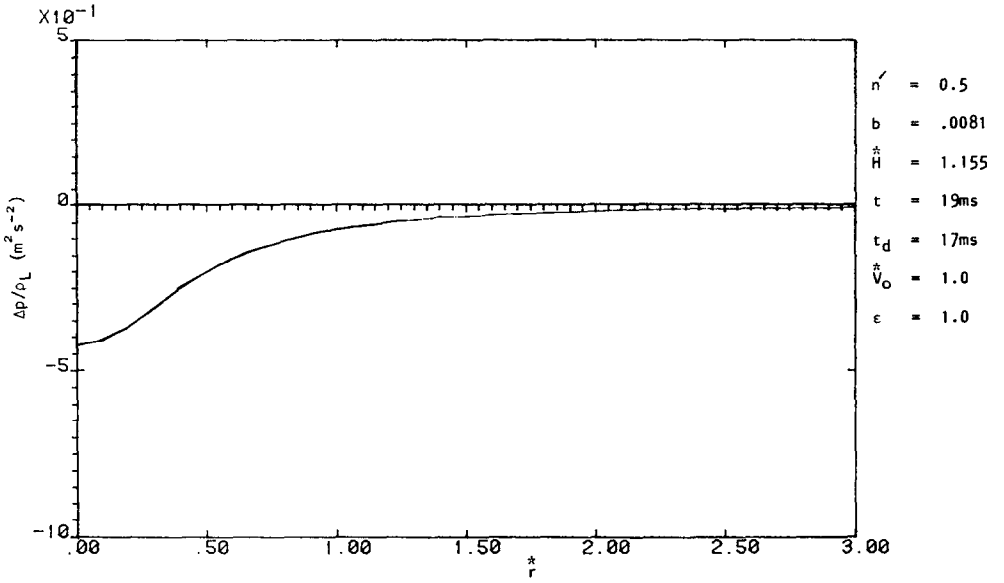

FIG. 13. Variation of Δp on the solid plane for various values of r^*.

will still be possible for a bubble to depart from the surface under reduced or non-buoyant gravity forces.

For positive rates encountered in saturated boiling regimes ($0.25 < n' < 0.75$), there is a high restraining force, $\mathbf{F}_n$, associated with the higher values of n'. This suggests that higher values of n' tend to promote the transformation of the boiling regime from nucleate to film boiling by enhancing the chance of coalescence due to prolonged departures. For a bubble growing in an infinite fluid, equation (A49) indicates that f_p and hence Δp will be negative if $n' < 0.4$. In the presence of a solid plane, an increasing portion of the lower part of the bubble becomes subjected to a negative value of Δp as n' falls below 0.5. This however does not become completely negative until n' becomes about 0.33. Thus the solid plane delays complete bubble collapse, i.e. it is possible for bubbles to continue to grow at a relatively reduced pressure difference Δp. The reduction compared to the infinite case is about 7.5%.

Figure 6 shows that for the case $n' = 0.75$, the pressure difference at the bubble top is nearly 14 times that for a bubble growing in an infinite liquid while for $n' = 0.5$ this value is four times. Thus the pressure distribution for a bubble with a large growth rate tends to flatten the top of the bubble. However the spherical shape assumed for the bubble may depart considerably from the real bubble shape and the results must be taken as indicative of the trend rather than accurate results.

For values of n' just under 0.5, the pressure difference is negative near the bubble base and remains positive

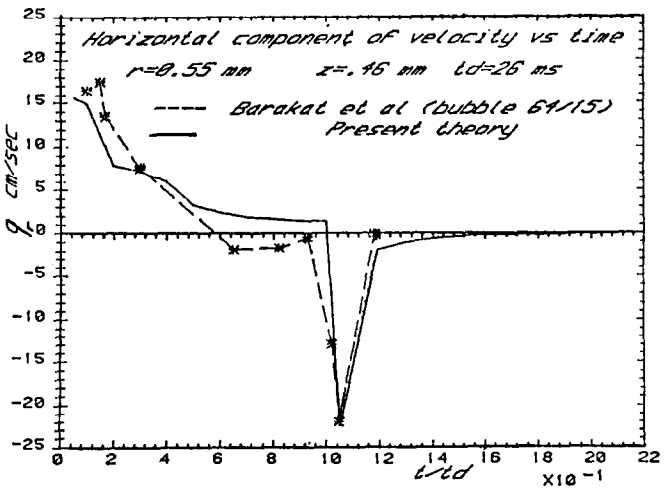

FIG. 14. Horizontal component of velocity vs time. $r = 0.55$ mm, $z = 0.46$ mm, $t_d = 26$ ms.

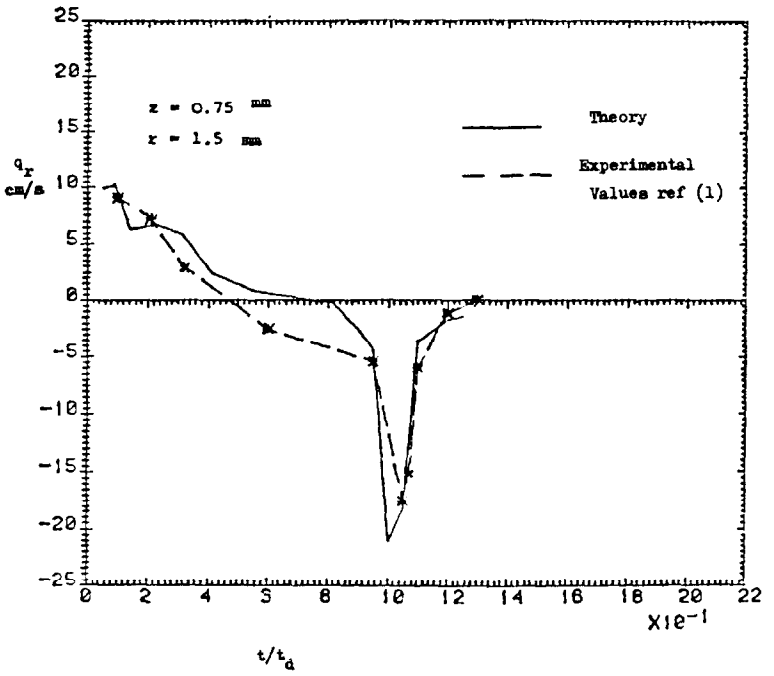

FIG. 15. Comparison between experimental values for bubble B and theoretical valves.

near the top of the bubble. Thus the lower part tends to be 'pushed in' or squeezed. This might be responsible for the often-reported 'mushroom shaped' bubbles. It will also enhance the bubble 'necking' process occurring near bubble departure time.

Figure 12 shows the variation of pressure at the nucleation site of a spherical bubble as a function of bubble height, H^*, while Fig. 13 shows the variation of pressure on the solid plane produced by the same bubble 2 ms after its departure. From these figures it can be seen that the nucleation site is subjected initially to a negative pressure difference. As H^* increases this becomes zero ($H^* = 1.67$ for $V_0^* = 1$) and from there on increases to a maximum positive value followed by a rapid decrease to zero again. The maximum values of the pressure excess occur at $H^* = 1.95$ for $V_0^* = 1$.

The initial pressure deficit will lead to an increase of pressure drop across the liquid interface encompassing the nucleation site, thereby enhancing bubble formation. On the other hand, the subsequent pressure excess tends to retard bubble formation at the nucleation site. This suggests that a second bubble will either form at the site during the period of pressure deficit or after the pressure becomes zero again following the maximum positive pressure drop. Judd *et al.* [12], report that bubble emission at a nucleation site is capable of either initiating or terminating bubble emission at a neighbouring site and they provide photographic evidence in support of this. Figure 13 shows the variation of $\Delta p/\rho_L$ with r^* on the solid surface. It can be seen from this that an initial pressure deficit extends to about three times the bubble radius. However, the effective region seems to lie in the region of 0 to 1.5 times the bubble radius. Thus the bubble departure and subsequent acceleration promotes bubble formation during the initial pressure deficit in a region which extends to nearly 1.5 times the bubble radius. This makes it easier for another bubble to grow on a site within this region (as the pressure drop required for the bubble growth is lowered due to the drop in the pressure of the liquid at the site). The excess (positive) pressure drop should lead to an effect opposite to that described for the deficit (negative) pressure drop. Thus it would appear that bubbles forming at a given nucleation site will tend to form in rapid succession but once stopped a lull period (corresponding to the duration of the excess pressure drop) must lapse before bubble generation at the site commences once more. This pressure differential cycle has wider engineering applications, see ref. [14], such as in the theory of fluidized beds and leakage through sieve trays.

Figures 8–11 give some flow parameters for a bubble translating on the plane according to equation (A1). In these figures, θ_0 is taken over the range $0 < \theta_0 < 2\pi$. The values given are calculated on the bubble surface $\rho_0^* = 1$, for selected values of ψ_0 which are given in the legends associated with these figures.

From Fig. 10, one can see that the pressure factor, f_p, and hence the pressure drop is minimum at the bubble base, $\theta_0 = \pi$, and that the pressure drop is negative at bubble base and top ($\theta_0 = 0$). Thus the fluid tends to move towards the top and bottom of the bubble with a larger tendency to move towards the bubble lower part.

From Figs. 8 and 9 it can be seen that the flow pattern over the bubble surface is a very complicated one indeed.

The thrust coefficient, C_f, has been calculated for three values of m, viz. $m = 1, 2$ and 5. The variation of C_f with n' for these cases is given in Fig. 11. From this it is clear that there is a positive force (accelerating the bubble in a direction away from the wall) acting on the bubble due to the translation of the latter on the plane. Thus it would be possible for a bubble to leave the surface even under negative gravity if it translates on the plane in a way that makes $\mathbf{F}_n$ large enough to counterbalance the restraining forces.

For a bubble growing in water (under atmospheric conditions) according to the growth law expressed by equation (A17) and taking the value of the parameter a in equation (A18) as $\sqrt{\pi}$, see ref. [5], and J_a (Jacobs number) as 100, equation (A5) gives a departure time of nearly 30 ms for a growth index, n', equal to 0.60. Compared to the experimental results of Cole and Shulman, ref. [16], the above value constitutes about 60% of the actual departure time. One must remember that equation (A51) ignores factors such as drag, deviation from the assumed spherical shape and effect of other bubbles. However, the above value emphasizes the importance of $\mathbf{F}_n$ in any serious attempt to calculate the departure time.

Figures 14 and 15 compare theoretical results based on the theory presented here and the experimental values of the horizontal velocity component, q_r, given in refs. [1] and [11]. The agreement between the predicted and the experimental values is reasonably good except near departure time (t/t_d nearly equal to 1). In this region the shape of the bubble no longer conforms to the spherical shape. This and 'bubble-necking' partially account for the discrepancies in the abscissae of Figs. 14 and 15. The reason that the theoretical model is able to predict the negative velocity during the 'necking period' is that the height of the bubble centre is taken somewhat larger than the radius of the bubble which in turn is taken as that of a bubble of spherical shape having the same volume as the bubble in question. So the theoretical model computes values of q_r as if the bubble is a small distance above the solid plane. However, it must be emphasized that the theoretical model is unable to predict the actual liquid behaviour satisfactorily during the 'necking period'.

4. CONCLUSIONS

From the foregoing discussion one may briefly conclude that:

(a) The presence of the solid plane allows a bubble to grow with a pressure excess which is about 7.5% less than that for a bubble growing in an infinite fluid under saturated boiling conditions.

(b) The total kinetic energy imparted to the liquid by a non-translating bubble growing on the solid is about 4.6 times that of a particle having the same mass as the liquid displaced by the bubble and moving with a velocity equal to the bubble growth rate. The total kinetic energy imparted to the liquid by a bubble growing on the solid is about 53% higher than that imparted to the liquid by a bubble growing in an infinite liquid. These values are important in all analysis using an energy balance.

(c) The flow pattern around the bubble surface may lead to arrest of bubble growth in subcooled boiling.

(d) The pressure distribution around the bubble produces a net force which tends to keep the non-translating bubble attached to the surface for $n' > 0.23$ and accelerate it in a direction away from the surface for $n' < 0.23$. This means that under conditions of strong subcooling a bubble will be able to depart from the surface even under zero or non-buoyant gravity fields.

(e) After bubble departure from the surface, the nucleation site is initially subjected to a negative pressure difference followed by a positive pressure difference which lasts for a period longer than that for the negative pressure but decreases to zero rapidly. This pressure effect extends over a distance about 1.5 times the bubble instantaneous radius on the solid plane. The negative pressure difference helps bubble growth while the positive pressure drop retards bubble growth. This mechanism might be partly responsible for the delay observed between successive bubbles from a site.

(f) A bubble translating on the plane experiences a repulsive force which tends to accelerate it in a direction away from the solid plane. Thus a sliding bubble growing on a solid plane can leave the plane even under zero or negative gravity fields. On the other hand if the sliding bubble starts collapsing the direction of this force is reversed and the sliding velocity must become zero before the bubble can depart.

(g) For non-translating bubbles, the pressure difference at the top tends to flatten this part of the bubble while for slower growing bubbles ($n' = 0.4$ to 0.45) the pressure distribution tends to produce a mushroom shaped bubble.

(h) The bubble hydrodynamic influence is shown to depend on both the bubble radius and rate of growth and as such it varies with time. This also means that it depends on the same factors that determine the bubble size and its rate of growth, that is on the Jacob number and the growth index n'. As $dR/dt = n'R/t$ (from $R = bt^{n'}$), then the effect produced inside a given area of influence varies directly with R and inversely with time.

(i) Although the theoretical work presented compares well with published experimental values, the theoretical prediction of liquid flow near bubble departure is not satisfactory. This is mainly due to distortion of the bubble shape and necking (elongation near the bubble base which makes the bubble shape resemble that of a pear).

Acknowledgements—The authors are grateful for the use of the facilities of the Department of Mechanical Engineering, Heriot-Watt University. This work was conducted while the first author was sponsored by the University, as Research Associate.

REFERENCES

1. M. A. Abdelghaffar, Asymmetric flow fields about bubbles with applications to nucleate boiling. Ph.D. thesis, Heriot-Watt University, U.K. (1982).
2. S. Kotake, On the mechanism of nucleate boiling, *Int. J. Heat Mass Transfer* **9**, 711–728 (1966).
3. C. P. Witze *et al.*, Flow about a growing sphere in contact with a plane surface, *Int. J. Heat Mass Transfer*, **2**, 1637–1652 (1968).
4. A. M. Judd, Calculations of the motion of a spherical bubble near a plane surface. CUED/A Thermo/TR3, Department of Engineering, Cambridge University, U.K. (1973).
5. R. Best *et al.*, Die warmeubertragung beim siden dem einfluss hydrodynamischer. *Int. J. Heat Mass Transfer* **18**, 1037–1047 (1975); also see English translation in *Heat Transfer in Boiling*, edited by E. Hahne and U. Grigull. Academic Press (1977).
6. S. Barakat, Flow patterns and heat transfer in pool barbotage. Ph.D. thesis, University of Manitoba, Winnipeg, Canada (1977).
7. B. I. Nigmatulin *et al.*, Effect of the interaction between vapour bubbles on the hydrodynamics and heat mass transfer of vapour–liquid flows, *Heat Transfer—Sov. Res.* **12**, (1980).
8. E. G. Keshock *et al.*, Forces acting on bubbles in nucleate boiling under normal and reduced gravity conditions, NASA report TN D-229 (1964).
9. H. D. Mendelson, The prediction of bubble terminal velocities from wave theory. *A.I.Ch.E. Jl* **13**, 250–253 (1967).
10. J. W. S. Rayleigh, *Philosophical Mag.* XXXIV.94 (1917); cited in H. Lamb, *Hydrodynamics*, p. 122. Dover, New York (1945).
11. S. Barakat *et al.*, Liquid flow patterns about barbotage bubbles, *J. Multiphase Flow* **3**, 383–397 (1977).
12. R. L. Judd, *et al.*, The nature of nucleation site interaction, *J. Heat Transfer* **102**, 461 (1980).
13. D. B. R. Kenning *et al.*, Fully developed nucleate boiling: overlap of areas of influence and interference between bubble sites, *Int. J. Heat Mass Transfer* **24**, 1025 (1981).
14. G. J. Jameson *et al.*, Pressure behind a bubble accelerating from rest: simple theory and applications. *Chem. Engng Sci.* **22**, 1053–1055 (1967).
15. M. Shiffman, On the best location of a mine near a sea bed, *Underwater Explosion Research*, Vol. II. U.S. Office of Naval Research (1950).
16. R. Cole *et al.*, Bubble departure diameters at subatmospheric pressures, *Chem. Engng Prog. Symp. Ser.* No. 62, 6 (1966).
17. A. M. Golovin *et al.*, Calculation of the rate of settling of homogeneous suspensions, *Prikl Mati Mekh* **1** (1978), mentioned in ref. [7].

APPENDIX

Flow-field due to non-spiralling motion of a spherical bubble

When the centre of mass of a bubble moves in a non-spiralling path with a velocity **V**, then its motion can be written in terms of a cylindrical frame of reference (r, ψ, z), such as the one shown in Fig. 1, as

$$\mathbf{V} = V_r \mathbf{e}_r + V_z \mathbf{e}_z \tag{A1}$$

$\mathbf{e}_r$ and $\mathbf{e}_z$ are unit vectors in the direction of positive r and z respectively. V_r and V_z are the components of **V** in the r and z directions respectively.

Let the height of the bubble centre above the heating surface be H and its angular position ψ_c as shown in Fig. 1. By making use of the following non-dimensionalized quantities.

$$r^* = r/R; \quad z^* = z/R; \quad V_r^* = V_r/\dot{R}; \quad V_z^* = V_z/\dot{R};$$
$$H^* = H/R; \quad \Phi^* = \Phi/R\dot{R}; \quad r_c^* = r_c/R \tag{A2}$$

and the recursive relations

$$f_n^* = \frac{1}{2H^* - f_{n-1}^*}$$
$$\mu_n^* = -\mu_{n-1}^* f_n^{*3} \tag{A3}$$
$$f_0^* = 0; \quad \mu_0^* = 1$$

then the results of ref. [1] give for this case

$$\Phi^* = \frac{S_0}{2S_1^{3/2}} + \frac{S_2}{2S_3^{3/2}} + \varepsilon\left[\frac{1}{\sqrt{S_1}} + \frac{1}{\sqrt{S_3}}\right] + \frac{1}{2}\sum_{n=1}^{\infty} \mu_n^* \left[\frac{S_0'}{(S_1')^{3/2}} + \frac{S_2'}{(S_3')^{3/2}}\right] \tag{A4}$$

where

$$S_0 = (r^* \cos\psi - r_c^*)V_r^* + (z^* - H^*)V_z^*$$
$$S_1 = r^{*2} + r_c^{*2} - 2r^* r_c^* \cos\psi + (z^* - H^*)^2 \tag{A5}$$

$$S_0' = (r^* \cos\psi - r_c^*)V_r^* + (z^* - H^* + f_n^*)V_z^*$$
$$S_1' = r^{*2} + r_c^{*2} - 2r^* r_c^* \cos\psi + (z^* - H^* + f_n^*)^2 \tag{A6}$$

$$S_2 = (r^* \cos\psi - r_c^*)V_r^* - (z^* + H^*)V_z^*$$
$$S_3 = r^{*2} + r_c^{*2} - 2r^* r_c^* \cos\psi + (z^* + H^*)^2 \tag{A7}$$

$$S_2' = (r^* \cos\psi - r_c^*)V_r^* - (z^* + H^* - f_n^*)V_z^*$$
$$S_3' = r^{*2} + r_c^{*2} - 2r^* r_c^* \cos\psi + (z^* + H^* - f_n^*)^2 \tag{A8}$$

$$\varepsilon = \frac{\rho_L - \rho_g}{\rho_L}. \tag{A9}$$

Since the direction ψ_c is constant, no spiralling motion, ψ_c has been taken as zero with no loss of generality. Here Φ^* is being evaluated at the point $P(r^*, \psi, z^*)$.

In deriving equation (A4), the following boundary conditions were used:

(a) The component of the velocity normal to the solid plane vanishes at all points on this plane.

(b) The potential function is taken to be zero at points far removed from the bubble.

(c) The normal component of the velocity, referred to a fixed origin, at any point on the bubble surface is equal to the sum of the fluid velocity induced by the bubble growth and the component of the velocity vector describing the motion of the bubble centre resolved along the normal to the surface at the point in question.

Initially the expression for the potential function describing the flow field due to two spherical cavities in general motion and satisfying boundary conditions (b) and (c) was derived using a multiple singularity technique generally employed for this class of problems and referred to as 'multiple reflections'. The case for the single bubble in the presence of the solid plane was then treated as a special case since boundary condition (a) is satisfied if the bubble is reflected in the solid plane. The expression given by the third term on the RHS of equation (A4) is due to the bubble growth while that under the summation sign ensures that the boundary conditions are met as the bubble gets very close to the solid surface or touches it. As the bubble moves away from the solid plane, the significance of the terms under the summation sign in (A4) diminishes. This is discussed in more detail in section (3) of this paper.

Figure 2 shows the variation of μ_n^* with n for the case $H^* = 1$, i.e. bubble touching the plane. It can be seen that the infinite series in equation (A4) converges very rapidly ($n \approx 15$). For other values of $H^* > 1$, the rate of convergence is greater.

The time is now opportune to consider in some detail two cases which are of considerable practical importance. These are:

(a) Bubble moving in a direction normal to the solid plane, i.e. $V_r^* = 0$.

(b) Bubble moving as described by equation (A1) with $H^* = 1$, i.e. sliding along the solid plane.

Bubble moving with a velocity normal to the solid plane

For this case $V_r^* = 0$ and r_c^* can also be taken as zero due to the axisymmetric nature of the flow field (symmetrical about z-axis).

Let the non-dimensionalized velocity components q_r^* and q_z^* be defined as

$$q_r^* = q_r/\dot{R}$$
$$q_z^* = q_z/\dot{R} \tag{A10}$$

q_r and q_z being the components of $\mathbf{q}$ in the r and z directions. Now by using equations (3) and (A4) one gets

$$q_r^* = \frac{3}{2} r^* V_z^* [BD^{-5/2} - AC^{-5/2}] + \varepsilon r^* [D^{-3/2} + C^{-3/2}] + \frac{3}{2} r^* V_z^* \sum_{n=1}^{\infty} \mu_n^* [B_1 D_1^{-5/2} - A_1 C_1^{-5/2}] \tag{A11}$$

$$q_z^* = \frac{1}{2} V_z^* [r^{*2} - 2A^2] C^{-5/2} - (r^{*2} - 2B^2) D^{-5/2}] + \varepsilon [BD^{-3/2} + AC^{-3/2}] + \frac{1}{2} V_z^* \sum_{n=1}^{\infty} \mu_n^* \times [C^{-5/2}(r^{*2} - 2A_1^2) - (r^{*2} - 2B_1^2) D^{-5/2}] \tag{A12}$$

where

$$A = z^* + H^*; \quad A_1 = z^* + H^* - f_n^* \tag{A13}$$

$$B = z^* - H^*; \quad B_1 = z^* - H^* + f_n^* \tag{A14}$$

$$C = r^{*2} + (z^* + H^*)^2; \quad C_1 = r^{*2} + (z^* + H^* - f_n^*)^2 \tag{A15}$$

$$D = r^{*2} + (z^* - H^*)^2; \quad D_1 = r^{*2} + (z^* - H^* + f_n^*)^2. \tag{A16}$$

In nucleate boiling the bubble radius is usually expressed in the form

$$R = bt^{n'} \tag{A17}$$

where t is the time measured from instant of bubble formation, n' is the growth index and b is a quantity which depends on the thermodynamics of the boiling regime and is normally written as

$$b = a\sqrt{\alpha_L} J_a \tag{A18}$$

where a is a constant α_L is the thermal diffusivity of the liquid being boiled and the quantity J_a is known as the Jacob's number, defined as

$$J_a = \frac{\rho_L C_l (T_l - T_s)}{\rho_g h_{fg}} \tag{A19}$$

where C_l and T_l are the specific heat and absolute temperature of the liquid, T_s is the absolute superheat temperature of the liquid at the system pressure and h_{fg} is the latent heat of vapourization of the liquid.

When the bubble detaches itself from the heating surface and starts its upward journey, the height H and the velocity V_z can be determined using expressions such as those suggested by Best *et al.* [5], viz.

$$H = R + V_{z\infty}(t - t_d) + \frac{[e^{-C(t-t_d)}] - 1}{C} \tag{A20}$$

$$V_z = [1 - e^{-C(t-t_d)}] V_{z\infty} + V_0 \tag{A21}$$

t_d being the time from initiation, C is a constant which depends on the fluid being boiled (450 s^{-1} for water) and $V_{z\infty}$ is the steady-state (terminal) velocity which can be computed using expressions such as that suggested by Mendelson [9], viz.

$$V_{z\infty} = \left[\frac{\sigma}{R\rho_L} + gR\right]^{1/2} \tag{A22}$$

where σ is the surface tension and g is the acceleration due to gravity. The term V_0 in equation (A21) allows for the fact that at $t = t_d$, $V_z = V_0$.

To allow for the shear stress at the wall, let the corrected velocities q_{rc}^* and q_{zc}^* be defined as:

$$q_{rc}^* = q_r^* + f^*(\lambda)$$
$$q_{zc}^* = q_z^* + F^*(\lambda) \tag{A23}$$

where λ is defined as

$$\lambda = z/\delta \tag{A24}$$

and δ is the hydrodynamic boundary-layer thickness. Best *et al.* suggest a value for δ given by

$$\delta = \frac{3}{2} H^2 \sqrt{\frac{2\nu_L}{R^3 V_z}} \tag{A25}$$

where ν_L is the kinematic viscosity of the liquid.

From ref. [1]

$$f^*(\lambda) = a_0^*(1 - \lambda)^3 \tag{A26}$$

$$a_0^* = 3r^* V_z^* \left\{ \frac{H^*}{[r^{*2} + H^{*2}]^{5/2}} - \sum_{n=1}^{\infty} \frac{\mu_n^*(f_n^* - H^*)}{[r^{*2} + (f_n^* - H^*)^2]^{5/2}} \right\} - \frac{\varepsilon r^*}{[r^{*2} + H^{*2}]^{3/2}} \tag{A27}$$

$$F^*(\lambda) = \beta_1 \lambda (1 - \lambda)^3 \tag{A28}$$

$$\beta_1 = \delta^* \left\{ \frac{2\varepsilon(r^{*2} - 2H^{*2})}{(r^{*2} + H^{*2})^{5/2}} - 3H^* V_z^* \left(\frac{3r^{*2} - 2H^{*2}}{[r^{*2} + H^{*2}]^{7/2}} - \frac{3}{H^*} \sum_{n=1}^{\infty} \frac{\mu_n^*(H^* - f_n^*)(3r^{*2} - 2(H^* - f_n^*)^2)}{[r^{*2} + (H^* - f_n^{*2})]^{7/2}} \right) \right\} \tag{A29}$$

$$\delta^* = \delta/R. \tag{A30}$$

The pressure, p, at a given point in the fluid can be obtained by using the unsteady state form of Bernoulli's equation, i.e.

$$\frac{p}{\rho_L} + \frac{1}{2}|\mathbf{q}|^2 - \frac{\partial \Phi}{\partial t} = F(t) \tag{A31}$$

where $F(t)$ is a function of time only. Since at ∞, $p = p_\infty$ and $\mathbf{q} = 0$, $\Phi = 0$ then

$$F(t) = p_\infty$$

where p_∞ is the static pressure of the undisturbed fluid. Thus (A31) reads

$$\frac{\Delta p}{\rho_L} = \frac{p - p_\infty}{L} = \frac{\partial \Phi}{\partial t} - \frac{1}{2}|\mathbf{q}|^2. \tag{A32}$$

Now

$$|\mathbf{q}|^2 = q_r^2 + q_z^2 = \dot{R}^2(q_r^{*2} + q_z^{*2}) \tag{A33}$$

$$\frac{\partial \Phi}{\partial t} = \Phi^*(R\ddot{R} + \dot{R}^2) + R\dot{R}\frac{\partial \Phi^*}{\partial t}. \tag{A34}$$

From the results of ref. [1], one gets:

$$\frac{\Delta p}{\rho_L} = \Phi^*[\dot{R}^2 + R\ddot{R}] + \frac{1}{2}\dot{R}^2[(2r^* - q_r^*)q_r^* + (2z^* - q_z^*)q_z^* + 2D_n(V_z^* - H^*)] + R\ddot{R}C_n\alpha^*(a^* - V_z^*) + R\dot{R}\left[A_n \sum_{n=1}^{\infty} f_n^{*2}\left[\dot{f}_{n-1}^* - \frac{2\dot{R}(V_z^* - H^*)}{R}\right] + B_n \sum_{n=1}^{\infty} f_n^{*2}[3\mu_{n-1}^*\dot{f}_n^* - f_n^*\dot{\mu}_{n-1}^*]\right] \quad \text{(A35)}$$

with

$$A_n = \frac{1}{2}\sum_{n=1}^{\infty} \mu_n^* f_n^*[(r^{*2} - 2A_1^2)C_1^{-5/2} + (r^{*2} - 2B_1^2)D_1^{-5/2}] \quad \text{(A36)}$$

$$B_n = \frac{1}{2}V_z^* \sum_{n=1}^{\infty} (B_1 D_1^{-3/2} - A_1 C_1^{-3/2}) \quad \text{(A37)}$$

$$C_n = \frac{\Phi^*}{V_z^*} - \frac{\varepsilon}{V_z^*}(C^{-1/2} + D^{-1/2}) \quad \text{(A38)}$$

$$D_n = \varepsilon(BD^{-3/2} - AC^{-3/2}) - \frac{1}{2}V_z^*[(r^{*2} - 2A^2)C^{-5/2} - (r^{*2} - 2B^2)D^{-5/2}] - \frac{1}{2}V_z^* \sum_{n=1}^{\infty} \mu_n^* \times [(r^{*2} - 2A_1^2)C^{-5/2} + (r^{*2} - 2B_1^2)D_1^{-5/2}] \quad \text{(A39)}$$

$$\dot{f}_n^* = f_n^{*2}[\dot{f}_{n-1}^* - 2(V_z^* - H^*)\dot{R}/R]$$
$$\dot{\mu}_n^* = f_n^{*2}[3\mu_{n-1}^*\dot{f}_n^* - f_n^*\dot{\mu}_{n-1}^*] \quad \text{(A40)}$$

$$\dot{\mu}_0^* = \dot{f}_0^* = 0$$
$$\dot{V}_z^* = \dot{V}_z/\ddot{R} = \alpha^*. \quad \text{(A41)}$$

The force, $\mathbf{F}_n$, due to the pressure distribution on the bubble surface (assumed positive when acting in such a manner as to accelerate the bubble in a direction away from the plane) is given by

$$\mathbf{F}_n = \int_s \Delta p \cos\theta \, dS \quad \text{(A42)}$$

the integral being taken over the bubble surface and dS is an element of area. θ is the angle shown in Fig. 1 with

$$dS = 2\pi R^2 \sin\theta \, d\theta$$

then

$$\mathbf{F}_n = \pi R^2 \int_0^{\pi} \Delta p \sin 2\theta \, d\theta. \quad \text{(A43)}$$

For a bubble growing on the plane

$$H^* = V_z^* = 1; \quad \dot{f}_n^* = \dot{\mu}_n^* = 0$$

and equation (A35) reduces to

$$\frac{\Delta p}{\rho_L} = \Phi^*[\dot{R}^2 + R\ddot{R}] + \frac{1}{2}\dot{R}^2[q_z^*(2z^* - q_z^*) + q_r^*(2r^* - q_r^*)]. \quad \text{(A44)}$$

For n' constant with time equations (A17) and (A44) give

$$f_p = \frac{\Delta p}{\rho_L b^2 t^{2n'-2}} = \Phi^*[2n'^2 - n'] + \frac{1}{2}n'^2[(2z^* - q_z^*)q_z^* + (2r^* - q_r^*)q_r^*] \quad \text{(A45)}$$

where f_p is a pressure factor.

Also equation (A43) can be written in terms of a force factor, C_f, as

$$\mathbf{F}_n = 2\pi\rho_L b^4 t^{(4n'-2)} C_f \quad \text{(A46)}$$

$$C_f = \frac{1}{2}\int_0^{\pi}\left[\Phi^*[2n'^2 - n'] + \frac{1}{2}n'^2(2z^* - q_z^*)q_z^* + (2r^* - q_r^*)q_r^*\right] \sin 2\theta \, d\theta. \quad \text{(A47)}$$

It should be noted that for the case $n' = 1/2$, the terms containing Φ^* in equations (A45) and (A47) vanish.

For comparison purposes consider the case of a spherical bubble growing in an infinite body of superheated liquid. The motion is described by the Rayleigh equation (10) as

$$R\ddot{R} + 3/2\dot{R}^2 = \frac{\Delta p}{\rho_L}. \quad \text{(A48)}$$

After introduction of equation (A17), this leads to

$$f_p = \frac{n'(5n' - 2)}{2}. \quad \text{(A49)}$$

This reduces to zero for $n' = 0.4$ and for values of $n' < 0.4$ f_p, and hence Δp, is negative. This result will be discussed further later on in this paper.

If all the forces except $\mathbf{F}_n$ and the buoyancy force, F_b, are considered to be small at the instant of bubble departure, then a force balance gives

$$-F_b = \frac{4}{3}\pi R^3(\rho_L - \rho_g)g = \mathbf{F}_n \simeq \frac{4}{3}\pi R^3\rho_L g. \quad \text{(A50)}$$

Introduction of (A46) into (A50) gives the following expression for the bubble departure time, t_d

$$t_d = \left[-\frac{3b}{2g}C_f\right]^{1/(2-n')}; \quad C_f < 0 \text{ for } g > 0. \quad \text{(A51)}$$

To calculate the total kinetic energy of the liquid, E_e, due to the bubble motion (which is also important in the theory of cavitation, underwater explosions, etc) one notes that

$$E_e = \frac{1}{2}\rho_L \int_s \Phi \frac{\partial\Phi}{\partial n} dS \quad \text{(A52)}$$

where $\partial/\partial n$ denotes differentiation with respect to the outward normal and the integral is being evaluated over the entire liquid boundary S. However, since the liquid free surface is assumed to be at infinity, $\Phi = 0$, and since the value $\partial\Phi/\partial n$ is zero over the solid surface, one needs to evaluate the integral in (A52) over the bubble surface only. Let a fluid velocity component, q_ρ, be defined as

$$q_\rho/\dot{R} = q_\rho^* = q_r^* \sin\theta + q_z^* \cos\theta \quad \text{(A53)}$$

where the notation of Fig. 1 has been used. If one defines a dimensionless kinetic energy, E_e^*, as

$$E_e^* = \frac{E_e}{\rho_L R^3 \dot{R}^2} = \frac{\frac{2\pi}{3}E_e}{\frac{1}{2}M_L\dot{R}^2} \quad \text{(A54)}$$

where M_L is the mass of the liquid having the same volume as the bubble, then equation (A52) may be written as

$$E_e^* = -\pi \int_0^{\pi} \phi^* q_\rho \sin\theta \, d\theta. \quad \text{(A55)}$$

The quantity $1/2M_L\dot{R}^2$ is equal to the kinetic energy of a particle, of mass equal to that of the fluid displaced by the bubble, moving with a velocity equal to the bubble growth rate $\dot{R}$. If one writes for this equivalent particle

$$E_{ep} = \frac{1}{2}M_L\dot{R}^2 \quad \text{(A56)}$$

then (A54) gives

$$E_e = \frac{3\pi}{2} E_e^* E_{ep}. \tag{A57}$$

The integral in (A55) has been evaluated for the case of a bubble growing on a solid plane using an adaptive three-point Gaussian quadrature. E_e^* is found to be 9.65 for this case and agrees closely with that given in refs. [3] and [15]. This gives

$$E_e = 4.6E_{ep} \tag{A58}$$

which implies that the total kinetic energy of the liquid due to the bubble growth is 4.6 times greater than that of the equivalent particle.

For a bubble in an infinite fluid

$$q = \dot{R}R^2/\rho^2 \to q_\rho^* = 1/\rho^{*2}$$
$$\Phi = -R^2\dot{R}/\rho; \quad 1/\rho^* = -\phi^*.$$

So that on the bubble surface

$$E_e = \pi \int_0^\pi \sin\theta \, d\theta = 2\pi.$$

Hence from (A57)

$$E_e = 3E_p. \tag{A59}$$

Thus the ratio of the total kinetic energy imparted to the liquid by a bubble growing on a solid surface to that growing in an infinite fluid is

$$\frac{(E_e) \text{ solid surface}}{(E_e) \text{ infinite fluid}} = 1.533 \tag{A60}$$

where in (A60), it is tacitly assumed that the two bubbles have the same mass and rate of growth.

Bubble sliding along the solid plane

The motion due to a bubble translating along the solid plane is but a special case of the motion produced by a bubble moving in accordance with equation (A1). For this case equations (3) and (A4) give for the velocity components (q_r^*, q_z^*, q_ψ^*) the following expressions:

$$q_r^* = \frac{B[h_1 V_z^* - BV_r^* \cos\psi]}{2S_1^{5/2}} - \frac{A[V_r^* \cos\psi + h_1 V_z^*]}{2S_3^{5/2}}$$
$$+ \frac{\varepsilon h_1}{3}\left[\frac{1}{S_1^{3/2}} + \frac{1}{S_3^{5/2}}\right]$$
$$+ \frac{1}{2}\sum_{n=1}^{\infty} \mu_n^* \left\{\frac{B(h_1 V_z^* - B_1 V_r^* \cos\psi)}{S_1^{3/2}}\right.$$
$$\left. - \frac{A_1[A_1 V_r^* \cos\psi + h_1 V_z^*]}{S_3'^{5/2}}\right\} \tag{A61}$$

$$q_z^* = \frac{A(3V_r^* h_2 - 2AV_z^*) + h_3 V_z^*}{2S_3^{5/2}}$$
$$+ \frac{B(3V_r^* h_2 + 2BV_z^*) - h_3 V_z^*}{2S_1^{5/2}} + \varepsilon\left[\frac{B}{S_1^{3/2}} + \frac{A}{S_3^{3/2}}\right]$$
$$+ \frac{1}{2}\sum_{n=1}^{\infty} \mu_n^* \left[\frac{A_1(3V_r^* h_2 - 2A_1 V_z^*) + h_3 V_z^*}{S_3'^{5/2}}\right.$$
$$\left. + \frac{B_1(3h_2 V_r^* + 2B_1 V_z^*) - h_3 V_z^*}{S_1'^{5/2}}\right] \tag{A62}$$

$$q_\psi^* = -\left[\frac{[V_r^*(h_3 + r_c^* h_1) + B(3r_c^* V_z^* + BV_r^*)]}{2S_1^{5/2}}\right.$$
$$+ \frac{[A(AV_r^* - 3r_c^* V_z^*) + V_r^*(h_3 + r_c^* h_1)]}{2S_3^{5/2}}$$
$$+ \varepsilon r_c^*\left[\frac{1}{S_1^{3/2}} + \frac{1}{S_3^{3/2}}\right]$$
$$+ \frac{1}{2}\sum_{n=1}^{\infty} \mu_n^* \left\{\frac{V_r^*(h_3 + r_c^* h_1) + B_1(3r_c^* V_z^* + B_1 V_r^*)}{S_1'^{5/2}}\right.$$
$$\left.\left. - \frac{A_1(A_1 V_r^* - 3r_c^* V_z^*) + V_r^*(h_3 + h_1 r_c^*)}{S_3'^{5/2}}\right\}\right] \sin\psi \tag{A63}$$

where

$$h_1 = 3(r^* - r_c^* \cos\psi)$$
$$h_2 = r^* \cos\psi - r_c^*$$
$$h_3 = r^{*2} + r_c^{*2} - 2r^* r_c^* \cos\psi \tag{A64}$$

and the rest of the parameters are as before.

For the bubble translating on the plane the analysis in ref. [1] gives the following expression for the pressure distribution:

$$\frac{\Delta p}{\rho_L} = \Phi^*(\dot{R}^2 + R\ddot{R}) - \frac{1}{2}\dot{R}^2[(q_r^* + 2r^*)q_r^2 + q_z^*(q_z^* - 2r^*)$$
$$+ q_\psi^{*2} - 2M(V_r^* - r_c^*)] + KR\ddot{R}(\alpha_r^* - V_r^*) \tag{A65}$$

where

$$K = \frac{1}{2}h_2\left[\frac{1}{S_1^{3/2}} + \frac{1}{S_3^{3/2}} + \sum_{n=1}^{\infty} \mu_n^*\left(\frac{1}{S_1'^{3/2}} + \frac{1}{S_3'^{3/2}}\right)\right] \tag{A66}$$

$$M = \frac{h_1 BV_z^* + V_r^*(r_c^* S_1 + h_1 h_2) + h_1 B_1 V_z^*}{2S_1^{5/2}}$$
$$+ \frac{V_r^*(r_c^* S_3 + h_1 h_2) - h_1 AV_z^*}{S_3^{5/2}}$$
$$- \frac{1}{2}\sum_{n=1}^{\infty} \mu_n^* \left[\frac{V_r^*(r_c^* S_1' + h_1 h_2) + h_1 B_1 V_z^*}{S_1'^{5/2}}\right.$$
$$\left. + \frac{V_r^*(r_c^* S_3' + h_1 h_2) - h_1 A_1 V_z^*}{S_3'^{5/2}}\right]$$
$$+ 3\varepsilon h_2\left[\frac{1}{S_1^{3/2}} + \frac{1}{S_3^{3/2}}\right] \tag{A67}$$

and

$$\alpha_r^* = \frac{V_r^*}{\dot{R}}. \tag{A68}$$

Information regarding values of V_r^* and α_r^* is not available at present. However, if one adopts a simple expression for V_r in the form:

$$V_r^* = m \tag{A69}$$

then equation (A65) reduces to:

$$\frac{\Delta p}{\rho_L} = \Phi^*(\dot{R}^2 + R\ddot{R}) - \frac{1}{2}\dot{R}^2[(q_r^* - 2r^*)q_r^*$$
$$+ q_z^*(q_z^* - 2z^*) + q_\psi^{*2}]. \tag{A70}$$

If $(\rho_0, \theta_0, \psi_0)$ denote spherical coordinates of a point in the liquid with reference to the centre of the bubble as origin then on the surface of the bubble

$$\rho_0^* = \rho_0/R = 1$$
$$r_0^* = \sin\theta_0 \tag{A71}$$

where (z_0^*, r_0^*, ψ_0) are cylindrical with origin at centre of bubble.

The restraining force, $\mathbf{F}_n$, is given by

$$\mathbf{F}_n = R^2 \int_{\psi_0=0}^{2\pi} \int_{\theta_0=0}^{\pi} \Delta p \sin\theta_0 \cos\theta_0 \, d\theta_0 \, d\psi_0. \tag{A72}$$

Using the transformations

$$z^* = z_0^* + 1$$
$$r^* = (r_c^{*2} + r_0^{*2} + 2r_0^* r_c^* \cos\psi_0)^{1/2} \tag{A73}$$
$$\psi = \arccos \frac{(r^{*2} + r_c^{*2} - r_0^{*2})}{2r^* r_c^*}$$

one gets

$$\mathbf{F}_n = \rho_L (bt^{n'-1})^4 C_f \tag{A74}$$

$$C_f = \int_{\psi_0=0}^{2\pi} \int_{\theta_0=0}^{\pi} \Delta p \sin\theta_0 \cos\theta_0 \, d\theta_0 \, d\psi_0. \tag{A75}$$

SUR LE CHAMP D'ECOULEMENT GENERE PAR LA CROISSANCE D'UNE SPHERE AU VOISINAGE D'UN PLAN SOLIDE, AVEC APPLICATION A L'EBULLITION NUCLEEE

Résumé—On décrit une solution analytique exacte de l'écoulement potentiel produit par une cavité sphérique croissant au contact ou proche d'un plan solide. Les paramètres du champ d'écoulement sont donnés sous forme adimensionnelle et leurs caractéristiques sont examinées. La théorie est appliquée au cas d'une bulle idéale en ébullition nucléée. Des expressions sont obtenues pour le départ de la bulle, la distribution de pression autour de la bulle et sur le plan solide, l'effet de la translation de la bulle le long du plan solide sur les paramètres d'écoulement et l'énergie cinétique totale donnée au liquide. Le concept d'une 'aire d'influence' en ébullition nucléée est revu. On montre que ni cette aire ni l'effet hydrodynamique à son intérieur dû au mouvement de la bulle ne demeurent constants pendant la croissance de la bulle. Quand cela est possible on compare les résultats avec les données expérimentales.

EIN MONTE-CARLO VERFAHREN FÜR GERADLINIGE BERANDUNGEN MIT KONVEKTION

Zusammenfassung—Mit Hilfe der Lösung für die Temperatur am Scheitelpunkt eines Kreissektors wurde eine Monte-Carlo-Methode für die zweidimensionale stationäre Wärmeleitung an geraden Begrenzungen entwickelt. Die Lösung durch Reihenentwicklung, welche die Temperaturverteilung entlang des Kreisbogens und den konvektiven Wärmeaustausch entlang der beiden geraden Seiten beschreibt, wird mit der Lösung durch finite Differenzen verglichen, um die Zahl der für eine bestimmte Genauigkeit benötigten Reihenglieder festzustellen.

О ПОЛЕ ТЕЧЕНИЯ, ВЫЗВАННОГО РАСТУЩЕЙ СФЕРОЙ У ТВЕРДО ПОВЕРХНОСТИ, В ПРИМЕНЕНИИ К ПУЗЫРЬКОВОМУ КИПЕНИЮ

Аннотация—Описывается точное аналитическое решение для потенциального течения, вызванного сферической полостью, растущей в контакте или вблизи твердой поверхности. В безразмерной форме представлены параметры поля течения. Исследуются их характеристики. Теория применима к случаю идеализированного пузырька, зарождающегося при пузырьковом кипении. Получены условие отрыва пузырька, распределение давления вокруг пузырька и на твердой поверхности; исследовано влияние перемещения пузырька вдоль твердой поверхности на параметры течения и полную кинетическую энергию, передаваемую жидкости. Рассматривается понятие 'зоны влияния' при пузырьковом кипении. Показано, что ни эта зона, ни гидродинамический эффект внутри нее, вызванный движением пузырька, не остаются неизменными в процессе роста. Полученные результаты сравниваются с имеющимися экспериментальными данными.